On the restoration of translational invariance in the critical quantum Ising model on a Fibonacci chain

1992 J. Phys. A: Math. Gen. 25 5223

(http://iopscience.iop.org/0305-4470/25/20/006)

J. Phys. A: Math. Gen. 25 (1992) 5223–5241. Printed in the UK

On the restoration of translational invariance in the critical quantum Ising model on a Fibonacci chain

Malte Henkel† and András Patkós‡

† Département de Physique Théorique, Université de Genève 24, quai Ernest Ansermet, CH-1211 Genève 4, Switzerland

‡ Department of Atomic Physics, Eötvös University, Puskin utca 5–7, H-1088 Budapest VIII, Hungary

Received 27 November 1991, in final form 26 May 1992

Abstract. The spectra of quasiperiodically modulated quantum Ising chains are investigated. For moderate values of the modulation strength a unified approach, based on the lifting of the degeneracy between the left- and right-moving eigenmodes, is proposed. The local scaling behaviour reflecting partial restoration of translational invariance is established. Both the conformally invariant scaling for the lower modes and the multifractal scaling for the higher ones are described in terms of the same quantity. A simple but accurate calculational scheme is constructed, where the rearrangement in the level spectra is due to the interaction between left- and right-moving modes of the periodic system as induced by the quasiperiodic modulation.

1. Introduction

The effect of quasiperiodic modulations of the nearest-neighbour interaction in 1D quantum ferromagnetic Ising models on the onset of the magnetic long-range order has attracted considerable interest (see Doria and Satija 1988, Benza 1989, Satija and Doria 1988, You *et al* 1991). The common approach consists of analysing the equivalent one-fermion spectrum (Lieb *et al* 1961) on a sequence of periodic approximants, with increasing sizes of the infinite quasiperiodic Fibonacci chain.

The band structure of the allowed eigenvalues can be explored using a transfer matrix technique. This technique was used to find the criterion for the existence of a zero mode in the fermion spectrum, which is the signature for criticality (Benza 1989). For generalized models, the same analysis was performed by Benza *et al* (1990) and You *et al* (1991). The linearization of the map (depending on two-parameters) realized by the trace of the transfer matrix around its two possible limit cycles yielded two typical scaling dimensions, which span the support of the scaling dimensions appearing in the one-fermion spectrum (Benza and Callegaro 1990). The value $\nu = 1$ of the thermal correlation length critical exponent and the logarithmic divergence of the specific heat led to the conclusion (Doria and Satija 1988, Benza 1989, Iglói 1988) that the magnetic transition is in the 2D Ising universality class.

The approach based on the band structure fits well to a multifractal analysis (Halsey *et al* 1986) of the band widths in full analogy with the procedure used to analyse the localization phenomena occuring in the one-dimensional Schrödinger equation with a quasiperiodic potential (Kohmoto *et al* 1987). The most natural

0305-4470/92/205223+19$07.50

question to be asked is whether the magnetic phase transition is accompanied by some characteristic change in the features of the one-fermion eigenmodes (Satija and Doria 1989, Satija 1990, You *et al* 1991). No universal answer could be obtained so far. The change in the spectral features of the eigenfunctions seems to depend sensitively on the details of the quasiperiodic modulation.

In this paper, we want to investigate the compatibility of the multifractal nature of the one-fermion levels with the consequences of conformal invariance at the critical point of the system. The main motivations to our study are as follows.

First, it is part of the complete universality classification of a second-order phase transition, since *all* anomalous dimensions of a critical 2D spin system with a static and isotropic RG fixed point are completely described by the representation theory of the conformal group. They can be obtained from the lower part of the excitation spectrum by standard methods (for a review, see e.g. Henkel 1990). However, there are modifications of the perfect, i.e. unmodulated, Ising model which retain the critical exponent values $\nu = 1$ and $\alpha = 0$ and yet do not belong to the Ising universality class. These models are obtained from a different realization of conformal invariance (Henkel and Patkós 1987) or may even display strongly anisotropic scaling (McCoy and Wu 1973, Frachebourg and Henkel 1991).

Second, the one-particle spectrum of the continuum theory corresponding to the critical perfect Ising model consists of degenerate, massless, left- and right-moving excitations with definite momenta. This degeneracy describes the fact that the conformal symmetry is the direct product of two Virasoro algebras. It is at least partially lifted when the non-periodic modulations, which break in particular translation invariance, are turned on, in contradistinction to the cases mentioned above when just the conformal realization is changed.

Third, the double degeneracy of the critical one-fermion spectrum of the perfect Ising model should be recovered in the thermodynamic limit, at least for the lowest momentum modes, even in the presence of the quasiperiodic modulation. We shall trace the levels which are the left–right partners in the perfect model. The analysis of these doublet splittings reveals that the degeneracy will in general not be restored in the upper part of the spectrum. The lifting of the degeneracy, induced by breaking translation invariance is reproduced by an approximate analytic treatment. A multifractal analysis will show a continuous range of local scalings, which were not present in the conformal description. It is interesting that a study of these level splittings, whose calculation is relatively easy, shows similar characteristics as the band structure investigations performed so far (Doria and Satija 1988, Benza and Callegaro 1990, You *et al* 1991).

In section 2 we recall the simplest version of the quasiperiodic quantum Ising chain (Doria and Satija 1988) which is to be investigated in the present paper. We expect, however, the conclusions of our study to remain valid for more general models with quasiperiodic modulations. We shall present and discuss the basic features of the numerically obtained spectra.

In section 3, an approximate diagonalization scheme is described. The ideas underlying this approximation are analogous to the ones followed in calculating the effect of weak periodic potentials on degenerate electronic levels (see e.g. Ashcroft and Mermin 1976). Already the first two approximants give precise eigenvalues in a moderate neighbourhood of the perfect Ising model. This success allows us also to interpret the features of the eigenvectors in terms of our approximation.

In section 4 three types of local scaling are analysed, which occur in the most

characteristic parts of the spectra. For individual levels the restoration of translational invariance and, in the lower part of the spectrum, that of conformal invariance, is demonstrated.

The multifractal analysis of the left–right splittings is described in section 5. Finite-size effects and the dependence on the strength of the modulation are studied. We find characteristic differences between the multifractal spectra associated with the lower and upper part of the one-fermion spectrum. Conclusions are given in section 6.

2. The model and its one-fermion spectrum

Consider a chain whose sites are lettered by either A or B. The Fibonacci sequence S_l is obtained recursively by composing words S_{l-1} and S_{l-2} via $S_l = S_{l-1}S_{l-2}$ and $S_0 = B$, $S_1 = A$. The length of the sequence is given by the Fibonacci numbers $F_l = F_{l-1} + F_{l-2}$, with $F_0 = F_1 = 1$. Let $\mathcal{L}(n)$ denote the letter at the site n.

The quantum Hamiltonian of the transverse Ising chain for a system of size $N = F_l$ is (for a review on the Hamiltonian limit, see Henkel 1990)

$$H = -\sum_{n=1}^{N} [\lambda_n \sigma^x(n)\sigma^x(n+1) + \sigma^z(n)] \tag{2.1}$$

where

$$\lambda_n = \begin{cases} \lambda & \text{if } \mathcal{L}(n) = A \\ r\lambda & \text{if } \mathcal{L}(n) = B\,. \end{cases} \tag{2.2}$$

The σs are Pauli matrices and periodic boundary conditions are used. The coupling r will be referred to as the *'modulation strength'*. The critical point is, as found numerically by Doria and Satija (1988) and confirmed analytically by Benza (1989),

$$\lambda_c = r^{-1/\sigma^2} \tag{2.3}$$

where $\sigma = \lim_{l\to\infty} F_l/F_{l-1} = (\sqrt{5}+1)/2$ is the golden mean.

The application of the Jordan–Wigner transformation maps the model onto a quadratic fermion problem, with fermionic creation and annihilation operators c_i^+, c_i satisfying $\{c_i^+, c_j\} = \delta_{ij}$. The charge operator $Q = 1/2[1 - \exp(-i\sum_n c_n^+ c_n)]$ commutes with H and the spectrum of H can be classified into an even fermion number ($Q = 0$) and an odd fermion number ($Q = 1$) sector. The standard technique of Lieb *et al* (1961) reduces the eigenvalue problem of H to the diagonalization of the $N \times N$ matrix

$$M = \begin{pmatrix} 1+\lambda_1^2 & -\lambda_1 & & & & (1-2Q)\lambda_N \\ -\lambda_1 & 1+\lambda_2^2 & -\lambda_2 & & & \\ & -\lambda_2 & \ddots & \ddots & & \\ & & \ddots & \ddots & \ddots & \\ & & & \ddots & 1+\lambda_{N-1}^2 & -\lambda_{N-1} \\ (1-2Q)\lambda_N & & & & -\lambda_{N-1} & 1+\lambda_N^2 \end{pmatrix}. \tag{2.4}$$

The diagonalized Hamiltonian takes the form $H = \sum_k \Lambda_k(\eta_k^+\eta_k - \frac{1}{2})$, where the normalization of the Λ_k is chosen to be

$$\Lambda_k = \left(\frac{|r|\log r^2}{r^2-1}\right)^{-1} m_k^{1/2} \tag{2.5}$$

where $\{m_k\}$ is the set of eigenvalues of M. We shall refer to the one-fermion energies Λ_k as *'levels'* for brevity. It can be shown by studying the dispersion relation near $\Lambda = 0$ (at the $\lambda = \lambda_c$ critical point) that this normalization corresponds to a choice of energy-momentum units such that the 'speed of sound' is unity (Ceccatto 1989). This convention is going to be useful in connection with the discussion of conformal invariance (see section 4).

We have considered the critical model with the following modulation strengths: $r = 0.3, 0.9, 1.001, 1.01$ and 1.5. For finite lattices of sizes $N = F_4 = 5, \ldots, N = F_{17} = 2584$, the exact finite-lattice spectra were obtained for both charge sectors. We now give several important observations as recognized from the visual inspection of the spectra. As an example, consider the $r = 1.5$ critical spectrum for a lattice with $N = F_{17} = 2584$ sites in the $Q = 0$ sector (figure 1).

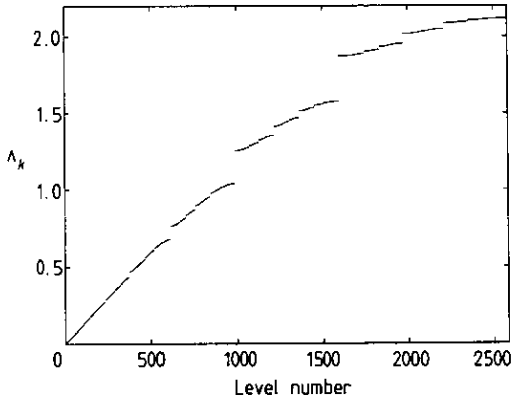

Figure 1. One-fermion energies Λ_k versus their level number, for $r = 1.5$ in the sector $Q = 0$ and $F_{17} = 2584$ sites.

(i) The dispersion curve for the critical $r = 1$ (perfect) quantum Ising chain is

$$\Lambda_k = 2|\sin k/2| \qquad k = \pm\frac{2\pi}{N}\left(m + \frac{1}{2}(1-Q)\right) \qquad m = 0, 1, 2, \ldots, \left[\frac{N}{2}\right] - 1 . \tag{2.6}$$

We shall label states by the quantum number

$$n = \begin{cases} 2m & \text{if } k \geqslant 0 \\ 2m + (1-2Q) & \text{if } k < 0 \end{cases} \tag{2.7}$$

and refer to n as *'level number'* and to m as *'pair number'*. From (2.6), Λ_k is a non-decreasing function of n (or m), if $r = 1$. This still holds true for $r \neq 1$, which means that there are no level crossings which would invalidate the grouping of levels into pairs by (2.7), at least for the values of r considered here.

(ii) There are some intervals in the energy range which are left empty and others which are very densely filled. We shall refer to these as *'gaps'* and *'bands'* throughout this paper, although the one-fermion spectrum is discrete for finite N. Comparison of figures 1 and 2 shows that the location and the width of the 'gaps' on the energy scale are almost independent of the lattice size. The longest chain displays a much richer hierachy of 'gaps', apparently uniformly distributed in the appropriate Λ intervals. We also note that the relative location of the 'gap' openings in the sequence can be associated with the same value $m/m_{\max}$ ($m_{\max} = [N/2] - 1$), and that they are located at those values of m which are determined by linear combinations of the lower Fibonacci numbers. The largest gaps occur at the relative positions F_{l-1}/F_l and F_{l-2}/F_l.

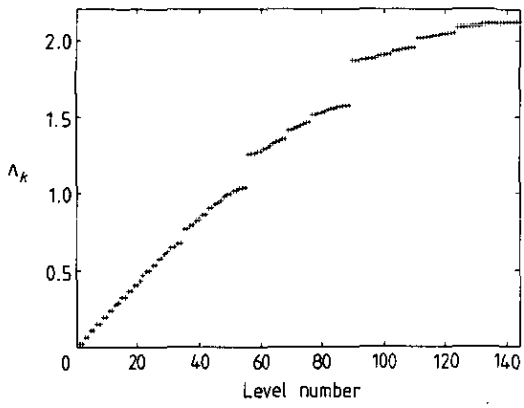

Figure 2. One-fermion energies Λ_k versus their level number, for $r = 1.5$ in the sector $Q = 0$ and $F_{11} = 144$ sites.

We shall ask the following questions. Do the eigenvalue gaps scale with the system size? What happens to the density of levels near the gap edges? In what sense can one define 'continuous spectra' in different parts of the spectrum?

(iii) The approximate representation (2.6) is working particularly well in the lower and almost linear part of the spectrum. Here one could expect the manifestation of conformally invariant patterns to be confirmed by precise quantitative checks.

(iv) On smaller lattices (figure 2), we recognize a doublet structure, at least in the lower part of the spectrum. We label the pairs by $(k, -k)$ (see above). The doublet splitting is much smaller than the gap between the subsequent pairs, although it is varying with k. In the sequel, whenever referring to *'doublets'* or *'(level or doublet) splittings'*, it will always be these doublets and their splittings which we have in mind. Those splittings whose label coincides with an odd Fibonacci number (or with an odd linear combination of some Fibonacci numbers) tend to become especially large. In figure 2, the largest splittings occur for the doublets labelled by $\#55 = F_9$ and $\#89 = F_{10}$. Can one associate the observed doublets with the $(k, -k)$ modes of the critical $r = 1$ Ising chain in the thermodynamic limit? If this is true in the lower part of the fermion spectrum, can we extend this interpretation for the doublets around F_{l-1} and F_{l-2}?

In the next section, we construct a hierarchical approximation scheme using the hypothesis that the levels are identifiable as deformations of the critical $r = 1$ Ising modes (see (2.6)). We shall see that even for the largest gaps, this approximation works very well.

3. A hierarchical approximation scheme

In this section we present a simple approximation scheme which allows, in spite of the apparent complexity of the problem, a precise representation of the numerical data. The main idea is to study the interaction between appropriately selected $(k,-k)$ pairs, generated by turning on the modulation in H. This amounts to diagonalization of M (2.4) in appropriately chosen subspaces.

The last of the observation listed in section 2 suggests that the exact eigenvectors of the $r = 1$ (perfect) case

$$\psi_j(k) = \frac{1}{\sqrt{F_l}} \exp \mathrm{i}k(j-1) \qquad k = \pm\frac{2\pi}{F_l}\left(m+\frac{1}{2}\right)$$

$$m = 0,1,\ldots,\left[\frac{F_l}{2}\right]-1 \qquad j = 1,2,\ldots,F_l \tag{3.1}$$

(we analyse the sector $Q = 0$) form a good basis for the diagonalization of M in which only a few off-diagonal elements are significant.

In figure 3 we show the 'intra-doublet' splittings for $N = F_{14} = 610$ and $r = 0.9$ between the $(k,-k)$ pairs as a function of k. The average of the splittings is small and of the order $\sim 10^{-4}$. Therefore a perturbative approach seems promising. Following the standard perturbative treatment of degenerate levels, we project M onto the two-dimensional subspace of the individual pairs and check whether this already reflects the main features of figure 3, namely the maxima in the *splittings* at specific m-values ($m = [F_{l-1}/2]$, $[F_{l-2}/2],\ldots$).

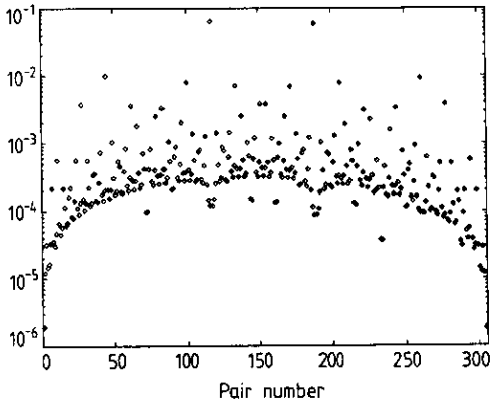

Figure 3. Exact intra-doublet splittings for $N = 610$ sites and $r = 0.9$ in the sector $Q = 0$.

For this we analyse the off-diagonal matrix elements of the difference $\delta M := M^{(r)} - M^{(r=1)}$ in the basis (3.1) (we hereafter always treat the sector $Q = 0$, unless otherwise stated) with $N = F_l$ sites

$$\langle k'|\delta M|k\rangle = \frac{1}{N}\sum_{n=1}^{N} \mathrm{e}^{\mathrm{i}(k-k')(n-1)}[(\lambda_n^2-1)+(1-\lambda_n)(\mathrm{e}^{\mathrm{i}k'}+\mathrm{e}^{-\mathrm{i}k})]\,. \tag{3.2}$$

3.1. Standard first-order perturbation theory

Consider first the standard degenerate perturbation theory of pairs $(+k,-k)$. From

$$\Lambda_{\pm k}=\left(\frac{|r|\log r^2}{r^2-1}\right)^{-1}\left(\frac{4\sin^2 k}{2}+\delta M_{k,k}\pm|\delta M_{k,-k}|\right)^{1/2} \tag{3.3}$$

one sees that the important quantity is ($N=F_l$)

$$\frac{1}{N}\Gamma(k):=\delta M_{k,-k}=\frac{1}{N}\sum_{n=1}^{N}e^{2ik(n-1)}[(\lambda_n^2-1)+2(1-\lambda_n)e^{-ik}]$$

$$=\frac{1}{N}\sum_{n=1}^{N}\tilde{\Gamma}(n)e^{2ik(n-1)}. \tag{3.4}$$

We now ask for which values of k $\Gamma(k)$ takes its largest values. Using the property

$$\tilde{\Gamma}_{F_l}(j)=\begin{cases}\tilde{\Gamma}_{F_{l-1}}(j) & j=1,\dots,F_{l-1}\\ \tilde{\Gamma}_{F_{l-2}}(j-F_{l-1}) & j=F_{l-1}+1,\dots,F_l\end{cases} \tag{3.5}$$

the following recursion relation is obtained:

$$\Gamma_{F_l}(k)=\Gamma_{F_{l-1}}(k)+e^{2ikF_{l-1}}\Gamma_{F_{l-2}}(k) \tag{3.6}$$

which can be rewritten in a matrix form

$$\begin{pmatrix}\Gamma_{F_l}(k)\\ \Gamma_{F_{l-1}}(k)\end{pmatrix}=\begin{pmatrix}1 & e^{2ikF_{l-1}}\\ 1 & 0\end{pmatrix}\begin{pmatrix}\Gamma_{F_{l-1}}(k)\\ \Gamma_{F_{l-2}}(k)\end{pmatrix}=\prod_{n=2}^{F_{l-1}}\begin{pmatrix}1 & e^{2ikF_n}\\ 1 & 0\end{pmatrix}\begin{pmatrix}\Gamma_{F_2}(k)\\ \Gamma_{F_1}(k)\end{pmatrix}. \tag{3.7}$$

In order to have a finite matrix element in the limit $F_l\to\infty$, the values of k should be chosen such that one (asymptotic) recursion step in (3.7) increases $\Gamma_{F_{l-1}}(k)$ by a factor of σ. Since this is just the feature of the mapping generating the Fibonacci numbers the requirement for the recursion matrix in (3.7) amounts to

$$\begin{pmatrix}1 & e^{2ikF_l}\\ 1 & 0\end{pmatrix}\to\mathcal{F}:=\begin{pmatrix}1 & 1\\ 1 & 0\end{pmatrix}\qquad l\to\infty. \tag{3.8}$$

The problem of selecting k such that (3.8) holds can be solved (Aubry *et al* 1988, Gähler 1991) by exploiting the asymptotic relationship between the Fibonacci numbers:

$$F_l\simeq\frac{1}{1+\sigma^2}(\sigma F_{l+1}+F_l)\qquad l\gg 1. \tag{3.9}$$

In order to write this in a geometrically transparent way, consider a sequence of vectors $\boldsymbol{X}=(F_{n+1},F_n)$ from a two-dimensional lattice. This sequence is generated by the Fibonacci mapping $\boldsymbol{X}_{n+1}=\mathcal{F}\boldsymbol{X}_n$. The eigenvectors of $\mathcal{F}$ are

$$e_{\parallel}=\frac{1}{\sqrt{1+\sigma^2}}(\sigma,1)\qquad e_{\perp}=\frac{1}{\sqrt{1+\sigma^2}}(-1,\sigma) \tag{3.10}$$

with the eigenvalues σ and $-1/\sigma$. In this basis, $\boldsymbol{X}$ is written as

$$\begin{aligned} \boldsymbol{X}_n &= X_{n,\parallel}\boldsymbol{e}_\parallel + X_{n,\perp}\boldsymbol{e}_\perp \\ X_{n,\parallel} &= \frac{1}{\sqrt{1+\sigma^2}}\left(\sigma F_{n+1} + F_n\right) \\ X_{n,\perp} &= \frac{1}{\sqrt{1+\sigma^2}}\left(-F_{n+1} + \sigma F_n\right) . \end{aligned} \tag{3.11}$$

The component $X_\perp$ vanishes exponentially under subsequent applications of $\mathcal{F}$. As a consequence one finds for the scalar product with an arbitrary vector $\boldsymbol{K}$

$$\boldsymbol{K}\cdot\boldsymbol{X}_l = K_\parallel X_{l,\parallel} + K_\perp X_{l,\perp} \to K_\parallel X_{l,\parallel} \simeq K_\parallel\sqrt{1+\sigma^2}F_l \qquad l\to\infty \tag{3.12}$$

where the asymptotic form of F_l has been used.

We now choose the vector $\boldsymbol{K}$ from the reciprocal lattice. Then the previous asymptotic statement is equivalent to

$$\exp\left(\mathrm{i}K_\parallel\sqrt{1+\sigma^2}F_l\right) \to \exp\left(\mathrm{i}\boldsymbol{K}\cdot\boldsymbol{X}\right) = 1 \qquad l\to\infty . \tag{3.13}$$

The smaller the $K_\perp$ component of the reciprocal lattice vector, the faster is the convergence and consequently, the larger will be the corresponding amplitude of the Fourier transform. The k-values to be considered are restricted to the interval $(0,\pi)$. The selection of those k-values for which the off-diagonal matrix element is large goes via

$$\begin{aligned} &\text{(i)} \quad K_\perp \quad \text{small} \\ &\text{(ii)} \quad 0 \leqslant 2k \simeq K_\parallel\sqrt{1+\sigma^2} < 2\pi \end{aligned} \tag{3.14}$$

(strict equality might not be always achievable since k is also quantized).

In the examples we describe below ($N = F_{14}, F_{17}$), one finds the following hierarchy for $F_l k/\pi = 2n+1$:

$$\begin{aligned} &\text{layer 1} \quad F_{l-1}, F_{l-2} \\ &\text{layer 2} \quad F_{l-4}, F_{l-2}\pm F_{l-6}, F_{l-1}\pm F_{l-6}, F_l - F_{l-4} \\ &\quad\vdots \qquad\quad \vdots \qquad\quad \vdots \qquad\quad \vdots \end{aligned} \tag{3.15}$$

such that the largest maxima of $\Gamma(k)$ occur for layer 1, the second largest for layer 2 and so on. We remark that this geometric consideration has been extended by Gähler to higher-dimensional recursive structures as well (Gähler 1991).

Equation (3.15) is valid if F_l is even. In this case, F_{l-1} and F_{l-2} are both odd and large gaps appear between the levels numbered by F_{l-1} and $F_{l-1}+1$ (F_{l-2} and $F_{l-2}+1$, respectively), which belong to the same pair. On the other hand, if F_l is odd, either F_{l-1} or F_{l-2} is even. For the even one, the gap appears between neighbouring pairs and the interaction between these two pairs must be taken into account.

In figure 4, the approximate doublet splittings are displayed as obtained numerically for $N = 610, r = 0.9$ from (3.3). The structure of the maxima and the average level of splittings is well reproduced, but the interesting fine structure of figure 3 is missing. In figure 5 we show the systematic change of the splitting pattern with increasing deviation of r from 1. Comparing figure 5(a) with figure 4, we note that first-order perturbation theory works well for r very close to unity. If $|r-1|$ gets larger, however, a new type of fine structure appears in the intra-doublet splittings which becomes more pronounced with growing $|r-1|$. For large values of $|r-1|$, the structure of the splittings changes completely. In figure 5(c), we observe a jump in the pattern around the pair number $[F_{l-2}/2]$. It is clear that these features are beyond the approximation treated so far.

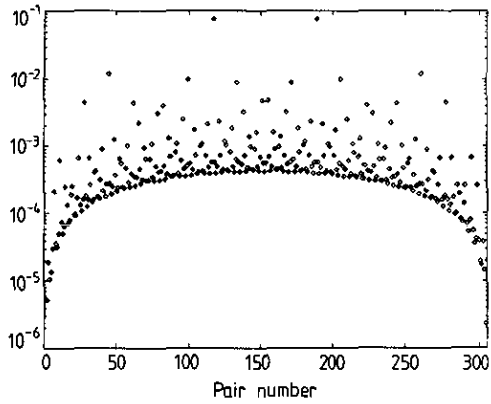

Figure 4. Intra-doublet splittings for $N = 610$ sites and $r = 0.9$ in the sector $Q = 0$ as obtained from first-order perturbation theory.

3.2. The hierarchical extension

In section 3.1 it was shown that the lowest-order perturbative approximation works well in the immediate neighbourhood of the perfect system. For finite but moderate values of $|r-1|$ one has to turn to systematic improvements. The scheme we are going to describe is not a direct extension of the first-order perturbation theory of section 3.1, but involves a projection mechanism onto a conveniently chosen subspace on which δM is diagonalized.

We have seen that the largest elements of δM occur at those k-values given by (3.15). The structure of δM is such that the size of its elements only depends on the difference of the states in k-space. Thus, if $2k_0$ is a k-value where the sum (3.4) takes one of its local maxima, then $\delta M_{k,k'}$ for the pairs (m is some integer)

$$\left[k = k_0 + \frac{2\pi}{F_l}\left(m + \frac{1}{2}\right),\ -k' = k_0 - \frac{2\pi}{F_l}\left(m + \frac{1}{2}\right)\right] \tag{3.16}$$

and

$$[-k, k'] \tag{3.17}$$

has the same value.

The largest off-diagonal matrix elements arise between those states whose level number differences are $2F_{l-1}$ or $2F_{l-2}$ and are thus given by layer 1 of (3.15). The

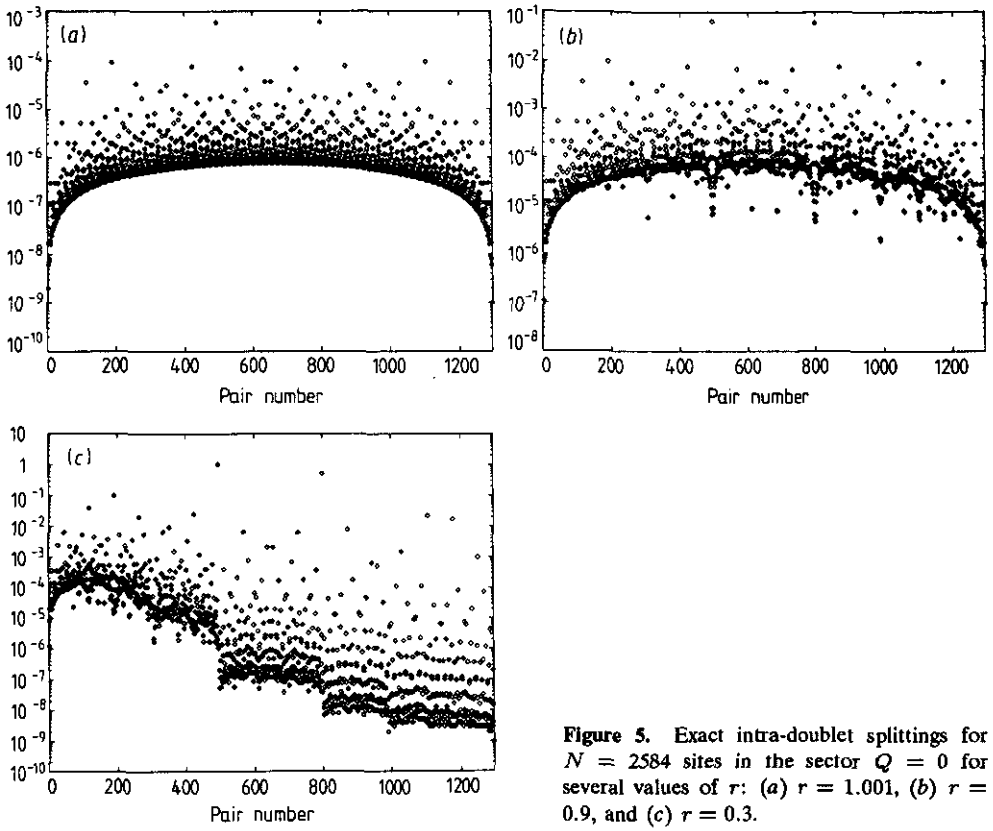

Figure 5. Exact intra-doublet splittings for $N = 2584$ sites in the sector $Q = 0$ for several values of r: (*a*) $r = 1.001$, (*b*) $r = 0.9$, and (*c*) $r = 0.3$.

second approximation, to be described below, will take these couplings into account. The group of second largest matrix elements is obtained between states related by layer 2 in (3.15) and so on. From figure 4, interpreted in the context of first-order perturbation theory (see section 3.1) it is indeed apparent that for the states of layer 1, the gaps are the largest. The group of second largest gaps is seen to occur at the places indicated by layer 2 in (3.15). The third layer of gaps in figure 4 seems to contain 16 entries. It becomes increasingly difficult to disentangle the layers belonging to lower grades of the hierarchy. However, since the matrix elements in the third layer are of order of some 10^{-2} smaller than those in the first, we expect that the scheme will converge rapidly, at least when $|r-1| \ll 1$.

We now give the states taken into the account for the first and second approximation in our hierarchical scheme. Consider the level structure in the neighbourhood of one of the largest gaps, e.g. F_{l-2}, with a k-value k^1.

The *first* approximation, denoted by 2×2, for the two levels of a degenerate doublet near F_{l-2} was obtained by diagonalizing separately 2×2 matrices coming from the pairs (we assume for convenience F_l even):

$$\left[k^1 = k_{F_{l-2}} + \frac{2\pi}{F_l}m,\ k^3 = -\left(k_{F_{l-2}} - \frac{2\pi}{F_l}m\right)\right] \tag{3.18}$$

and

$$\left[k^2 = -k^1,\ k^4 = -k^3\right]. \tag{3.19}$$

These pairs have level numbers differences of $2F_{l-2}$. In this way in the first approximation all doublets of the pairs labelled by (k^1, k^2) and (k^3, k^4) remain degenerate except the $m = 0$ doublets.

The *second* approximation, to be denoted by 8×8, also includes in the eigenvalue problem the levels which have a level number difference of (3.18) and (3.19):

$$\left[k^5 = -\left(k_{F_{l-1}+F_{l-3}} - \frac{2\pi}{F_l}m\right),\ k^7 = k_{F_{l-1}+F_{l-3}} + \frac{2\pi}{F_l}m\right] \tag{3.20}$$

and

$$[k^6 = -k^5,\ k^8 = -k^7] \tag{3.21}$$

and one has an 8×8 matrix formed from these four pairs. The results of the above projection are accurate to four or five digits and in figure 6 we show that this approximation correctly accounts for the fine structure of the splittings near the biggest gaps.

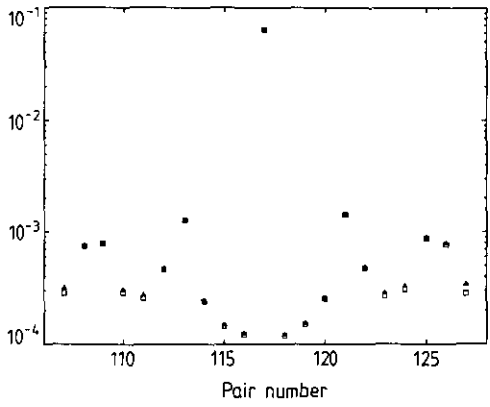

Figure 6. Comparison of the 8×8 approximation (triangles) and the exact result (squares) for the intra-doublet splittings for $r = 0.9$ and $N = 610$ sites in the $Q = 0$ sector, in the neighbourhood of the gap at $F_{l-2} = F_{12} = 233$.

For the next approximation step two types of problems can be addressed:

(i) The levels in the neighbourhood of the 'strongest' off-diagonal directions (F_{l-1}, F_{l-2}) can be improved by including those states whose level number differences with $k^1, \ldots, k^8$ are given by layer 2 of (3.15).

(ii) The neighbourhood of a 'second-order gap' $(F_{l-4}, \ldots, F_l - F_{l-4})$ can be studied by replacing in (3.18) and (3.19) $k_{F_{l-2}}$ by some k_G with G belonging to this layer $(F_{l-4}, \ldots, F_l - F_{l-4})$. Then the states with a level number difference given by layer 1 are to be included and the resulting 12×12 matrix is to be diagonalized.

These constructions can be continued to any degree of precision desired.

3.3. Eigenvectors

The wavefunctions of the near-edge levels in our approximation are finite linear combinations of extended Ising modes and thus are extended themselves. This result for the nature of the near-edge exact eigenvectors of (2.4) has been tested numerically. We find that for $r = 0.9$ all near-edge eigenvectors are extended. The states forming the gap precisely at F_{l-2} are characterized by $|\psi_n| \simeq \psi_{\text{ave}}$ on a dense subset of

the lattice points, where ψ_{ave} is some 'average value' of $|\psi_n|$. The variations of ψ_n around ψ_{ave} show a self-similar pattern of dips of decreasing depth. The eigenvectors of the doublets close to the gap can be described (for $F_l \gg 1$) by

$$\psi_{[F_{l-2}/2]+m}(j) \sim \cos(2\pi\sigma^{-2}j + \gamma)\cos\left(\frac{2\pi}{F_l}2mj\right) \tag{3.22}$$

(γ is in the context of our approximation the phase of the off-diagonal matrix element). This behaviour is the result of superposing high-frequency periodic approximants to quasiperiodic functions with nearly equal wavenumbers. The 'carrier wave' formed from our lowest-order approximate eigenvectors becomes in the $l \to \infty$ limit a true quasiperiodic function, which carries a periodic modulation. The wavelength of this modulation is $F_l/2m$, where m labels the distance of the doublets to the gap. This regularity can be observed to be satisfied by the exact eigenvectors near the gap edges.

The picture is completely different for $r = 0.3$. There we observe an abrupt change in the splitting pattern just at F_{l-2} (see figure 5(*c*)). The wavefunctions of the levels above the gap appear to be critical (neither extended nor localized). The proposed perturbative treatment is no longer applicable.

The success of our scheme in the quantitative description of the broad neighbourhood of the largest gaps is due to the strong interactions of the modes $(k_0 + k')$ and $-(k_0 - k')$ of the perfect Ising model, induced by the breakdown of translational invariance. The modulated quantum Ising chain might turn out to be a generic example of the physical mechanism for the gap formation in the spectra of general non-periodic systems.

The importance of the intra-doublet splittings in the proposed approximation scheme should convince the reader about the interest of analysing the intervals defined by the splittings with a multifractal approach, which will be presented in section 5.

4. Typical local scaling in the spectra

In the previous sections we have given a simple, but accurate interpretation of how gaps open between would-be degenerate left–right partners as a consequence of quasiperiodic modulation. Here we study the finite-size scaling behaviour of the levels, using the exact eigenvalues of H on finite lattices.

4.1. Gaps and near-gap levels

One finds gaps at some allowed combinations of Fibonacci numbers $\Phi = \sum_p c_p F_{l-p} < F_l$. A given gap is studied by keeping the c_p fixed while increasing l (compare figures 1 and 2). The local scaling index μ_{gap} of a gap is defined as

$$\lim_{l\to\infty}[\Lambda(\Phi+1) - \Lambda(\Phi)] \sim F_l^{-\mu_{\text{gap}}}. \tag{4.1}$$

In table 1 the l-dependence of the logarithms of the left-hand side of (4.1) is given for the gaps at level number $F_{l-p}, p = 1, 2, \ldots$. This particular set covers at least three orders of magnitude and can therefore be considered to be representative

of the hierarchy of gaps. A *non-uniform* convergence to a constant width can be observed. The gaps corresponding to even values of F_{l-p} form a separate sequence, converging slowly, while the sequence formed for the odd F_{l-p} converges rapidly. Both subsequences have the *same* limit. This is so since for F_{l-p} odd, the gaps are intra-doublet gaps, while for F_{l-p} even, they occur between doublets. This observation represents an extra argument for selecting the intra-doublet splittings as the natural mechanism for the formation of gaps. For an accurate extrapolation towards $F_l \to \infty$, one should discard the width estimates from F_{l-p} even. One finds up to $p \simeq 10$ that all gaps converge to some finite width, which implies

$$\mu_{\text{gap}} = 0 \,. \tag{4.2}$$

The constant value of the corresponding left–right splittings is a clear signal for the breakdown of translational invariance even in the critical point.

Table 1. Finite-lattice data for the logarithm of the intra-doublet gaps opening at F_{l-p} for various system sizes N, for $r = 0.9$ and $Q = 0$ and $F_l = F_{17} = 2584$. The entries labelled by * are those corresponding to inter-doublet splittings and should be discarded when extrapolating towards $N \to \infty$.

N	F_{l-1}	F_{l-2}	F_{l-3}	F_{l-4}	F_{l-5}	F_{l-6}	F_{l-7}	F_{l-8}	F_{l-9}	F_{l-10}
8	−2.803	−2.735								
13	−1.334*	−2.739	−3.777							
21	−2.819	−1.408*	−3.777	−4.603						
34	−2.820	−2.750	−1.782*	−4.597	−5.575					
55	−2.470*	−2.751	−3.796	−2.212*	−5.568	−6.517				
89	−2.822	−2.470*	−3.798	−4.614	−2.672*	−6.510	−7.481			
144	−2.822	−2.751	−3.095*	−4.617	−5.587	−3.144*	−7.473	−8.440		
233	−2.795*	−2.751	−3.799	−3.591*	−5.590	−6.528	−3.620*	−8.433	−9.403	
377	−2.822	−2.731*	−3.799	−4.617	−4.092*	−6.531	−7.492	−4.099*	−9.395	−10.365
610	−2.822	−2.752	−3.720*	−4.617	−5.590	−4.578*	−7.494	−8.451	−4.579*	−10.357
987	−2.821*	−2.752	−3.799	−4.457*	−5.590	−6.531	−5.060*	−8.454	−9.414	−5.060*
1597	−2.822	−2.750*	−3.799	−4.617	−5.229*	−6.531	−7.495	−5.541*	−9.416	−10.375
2584	−2.822	−2.752	−3.794*	−4.617	−5.590	−5.875*	−7.495	−8.454	−6.022*	−10.378

Using standard convergence-improving algorithms (Henkel and Schütz 1988) we find that the levels $\Lambda(F_{l-p}+1)$ and $\Lambda(F_{l-p})$ separately converge to finite limits as $l \to \infty$. Next, we have studied the finite-size scaling of the states whose label has a *fixed* distance from the edge states:

$$\Lambda(F_{l-p}+1+q) - \lim_{l\to\infty} \Lambda(F_{l-p}+1) \sim A_q F_l^{-\mu_{\text{edge}}} \,. \tag{4.3}$$

From the analysis, the data corresponding to even values of F_{l-p} were discarded. Table 2 shows the results of the extrapolation for $p = 1,2$ and $q = 1,2,3,4$, for $r = 0.9$ and $Q = 0$. First, the extrapolated values of μ_{edge} were found for all eight states and turn out to be

$$\mu_{\text{edge}} \simeq 2 \tag{4.4}$$

implying that the density of states behaves in a similar way as in the van Hove singularities. The amplitudes A_q were obtained using the individual exponents of table 2 and are listed in the same table as well. We see that for the pairs of states $(q = 1,2)$ and $(q = 3,4)$ the amplitudes agree within 5%. This is equivalent to the restoration of translational invariance *near* the gap edges! The quadratic relationship between the amplitudes of the subsequent doublets means that the continuum spectrum building up near the gap edges in the $l \to \infty$ limit will have a quadratic dispersion

$$\epsilon := F_l^2 \left[\Lambda(F_{l-p_0} + 1 + q) - \lim_{l\to\infty} \Lambda(F_{l-p_0} + 1) \right] \sim q^2 . \tag{4.5}$$

The equations (4.2), (4.4), (4.5) check numerically the exact results found with the method of limit cycles (Benza and Callegaro 1990).

Table 2. Estimates for the exponent μ_{edge} and the amplitude A_q for the convergence of the closest states (labelled by q, (4.3)) to the edge the gap opening at F_{l-p}. For the entry marked by * the finite-size data did not converge. The intrinsic extrapolation error for the A_q is at least 5 units in the last given digits. This does not yet contain possible systematic errors arising from the imprecise knowledge of μ_{edge}.

	μ_{edge}		A_q	
q	$p = 1$	$p = 2$	$p = 1$	$p = 2$
1	1.95 ± 0.05	2.00 ± 0.02	—*	383
2	1.99 ± 0.03	1.99 ± 0.02	196	400
3	2.00 ± 0.02	2.00 ± 0.1	760	1598
4	2.00 ± 0.03	2.00 ± 0.1	802	1659

4.2. Conformal scaling near $\Lambda = 0$

For the $\Lambda_k \to 0$ edge of the one-particle spectrum, the results of the conformally invariant perfect Ising model can be recovered, independent of the value of r $(\neq 0)$. For a conformally invariant system, the differences of the eigenvalues E_i of H are related to the scaling dimensions x_i via (Cardy 1984)

$$E_i - E_0 = \frac{F_l}{2\pi} x_i . \tag{4.6}$$

For the Ising model, all eigenvalues E_i can be written as a sum over some λ_k. This fixes the local exponent μ_{conf}:

$$\mu_{\text{conf}} = 1 . \tag{4.7}$$

Consequently, one considers the scaling amplitudes

$$A_k := \frac{F_l}{2\pi} \Lambda_k . \tag{4.8}$$

For the perfect $(r = 1)$ Ising model, the Λ_k are given by (2.6). The first eight A_k are given in table 3 for both $Q = 0$ and $Q = 1$ and were obtained by extrapolating finite-lattice data from $F_3 = 3$ to $F_{17} = 2584$ towards $F_l \to \infty$, using the BST extrapolation

algorithm (Henkel and Schütz 1988). We find that for all values of r, the result for the perfect Ising model is recovered. For $r = 0.9$, this was also checked for the levels 13, 14 and 21, 22. This means that the lower levels of the quantum Ising model on a Fibonacci chain can be associated with definite momenta, implying restoration of translation invariance, and they do form equidistant towers in agreement with conformal invariance. The values of the lowest dimensions, using (4.6), allow the recovery of the 2D Ising exponents $x_\epsilon = 2 - 1/\nu = 1$ and $x_\sigma = \beta/\nu = 1/8$. While the result for x_ϵ is in agreement with earlier conclusions (Doria and Satija 1988, Benza 1989, Iglói 1988), the confirmation for x_σ has not been carried out.

Table 3. Finite-size estimates for the eight lowest critical one-fermion energies Λ_k of the quantum Ising chain on the Fibonacci lattice for several values of r and in both charge sectors. The estimated error is expected to be of the order 3×10^{-5}. The exact result for $r = 1$ is taken from (2.6).

		μ_{edge}	A_q	
	$r = 1.0$	$r = 0.3$	$r = 0.9$	$r = 1.5$
$Q = 0$	1/2	0.500 00	0.500 00	0.500 00
	1/2	0.499 99	0.500 00	0.500 00
	3/2	1.499 97	1.500 00	1.500 00
	3/2	1.499 97	1.500 00	1.500 00
	5/2	2.500 01	2.500 00	2.499 99
	5/2	2.499 99	2.500 00	2.500 01
	7/2	3.500 01	3.499 99	3.500 01
	7/2	3.500 00	3.500 00	3.500 01
$Q = 1$	0	0.0	0.0	0.0
	1	1.000 00	1.000 00	1.000 00
	1	1.000 01	1.000 00	1.000 00
	2	1.999 99	2.000 00	2.000 00
	2	2.000 00	1.999 99	1.999 99
	3	3.000 02	3.000 00	2.999 44
	3	3.000 02	3.000 00	3.000 00
	4	3.999 80	4.000 00	3.999 98

5. Multifractal scaling of the left–right splittings

The local scaling exponents found in section 4, $\mu_{\text{gap}} = 0$, $\mu_{\text{edge}} = 2$, $\mu_{\text{conf}} = 1$ are just some examples of sets of one-fermion levels obeying different finite-size scaling behaviours. Since the left–right splittings respond in a characteristic way to the quasiperiodic modulation, it is of interest to investigate the multifractal scaling of these. Consider the ordered ascending sequence of left–right splittings ($Q = 0$ sector):

$$\omega_s = \Lambda(2s) - \Lambda(2s-1) \qquad s = 1, \ldots, \left[\frac{F_l}{2}\right]. \tag{5.1}$$

We choose to give equal weight to all pairs.

Following Halsey *et al* (1986), we define a 'partition function', from which we shall obtain the multifractal spectrum $f(\alpha)$

$$Z_l(q,\tau) := \sum_{s=1}^{[F_l/2]} \omega_s^{-\tau} \left[\frac{F_l}{2}\right]^{-q} . \tag{5.2}$$

By the convention proposed by Halsey *et al* (1986), one can fix $Z_l(q,\tau) = 1$. This yields a relation between q and τ. Assuming the local scaling

$$\omega_s \sim F_l^{-\mu_s} \tag{5.3}$$

the sum in (5.2) is dominated in the $F_l \to \infty$ limit by the region where $\mu\tau - q(\tau)$ is stationary:

$$\mu = \frac{\mathrm{d}q_l(\tau)}{\mathrm{d}\tau} . \tag{5.4}$$

The standard analysis is based on the inverse function of (5.4)

$$f_l(\alpha) := \alpha q - \tau_l(q) \qquad \alpha = \frac{1}{\mu} = \frac{\mathrm{d}\tau_l(q)}{\mathrm{d}q} . \tag{5.5}$$

By the typical local scaling seen previously we expect the support of $f(\alpha)$ to include the points $\alpha = 0.5, 1, \infty$. A few peculiar values of $f(\alpha)$ have a simple interpretation. For example, the maximum value of f is the fractal dimension D_0 of the support, while the value $D_1 := f(\alpha_1) = \alpha_1$ is referred to as information dimension.

In figure 7, the $f(\alpha)$ spectrum of the doublet splittings is shown in the sectors $Q = 0$ and $Q = 1$ for $r = 0.9$ on the chain with $N = F_{17} = 2584$ sites. The behaviour of the two curves on the segment $0.5 \leqslant \alpha \leqslant 1$ is Q-independent, the maxima are reached close to $\alpha = 1$. The contribution of the slowly decaying splittings with $\alpha > 1$ (the gaps are included here) is larger for the $Q = 0$ sector than for $Q = 1$. This should be a finite-size effect, however.

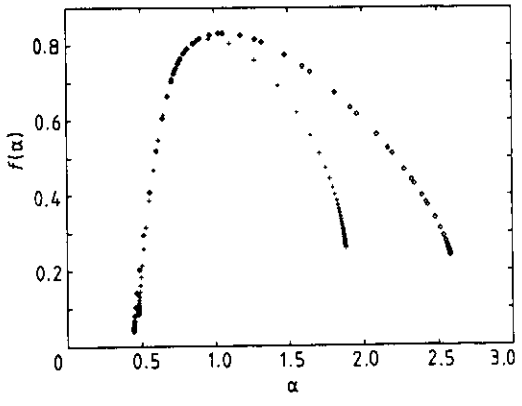

Figure 7. Comparison of the multifractal distribution function $f(\alpha)$ between the two sectors $Q = 0, 1$ for $r = 0.9$ and $N = 2584$ sites. ($Q = 0$: $\circ$, $Q = 1$: $+$).

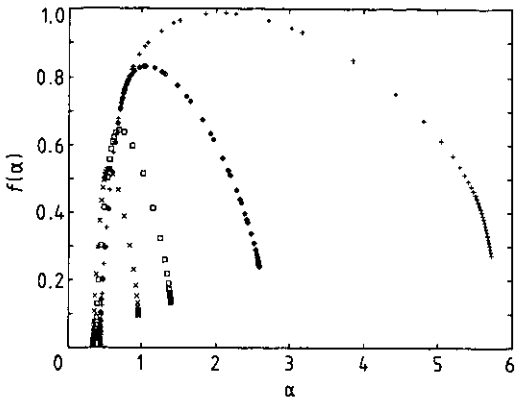

Figure 8. Comparison of the multifractal distribution function $f(\alpha)$ for several values of r and for the sector $Q = 0$ and $N = 2584$ sites. $r = 0.9$: $\diamond$, $r = 1.5$: $+$, $r = 1.01$: $\square$, $r = 1.001$: $\times$.

The r-dependence of the multifractal spectrum is displayed in figure 8. While r approaches the perfect value $r = 1$, the maximal value of $f(\alpha)$, $f(\alpha_0)$ decreases and α_0 shifts towards $\frac{1}{2}$. This is in agreement with the full restoration of translational invariance in the $r \to 1$ limit, since then all splittings are vanishing exactly. The largest lattice data hint towards a faster scaling ($\alpha_0 < 1$) than shown by the levels themselves ($\alpha = 1$).

This tendency for the restoration of translational invariance is *not* uniformly present in the spectrum. Following Benza and Callegaro (1990) we performed the multifractal analysis on the lower part of the spectrum ($1 \leqslant s \leqslant (F_{l-2}/2)$ in (5.2)) and on its upper part ($((F_{l-2}/2) + 1 \leqslant s \leqslant (F_l/2)$ in (5.2)) separately. We have found that $f(\alpha)$ calculated from the lower part for $N = 2584$ sites and $r = 0.9$ looks quite similar to the full spectrum at $r = 1.01$, implying that in the lower part the effect of the quasiperiodic modulation is weaker. In a careful study, Godrèche and Luck (1990) have adressed the possibility that finite-size effects might produce a spurious multifractal spectrum. As a criterion for the *absence* of multifractality in the large-N limit, they proposed that the curvature of the function $f(\alpha)$ close to its maximum should diverge logarithmically with the lattice size.

We find that the finite-size dependence of $f(\alpha)$ is very weak in the segment $0.5 \leqslant \alpha \leqslant 1$, as illustrated for the upper spectrum in figure 9. In particular, we do not see a divergence of the curvature. In the region $\alpha > 1$ however, $f(\alpha)$ depends strongly on the system size and also on the part of the one-fermion spectrum included into the analysis. The difference between the $f(\alpha)$ curves calculated either from the full spectrum or from its upper part appears to be a finite-size effect since the curves widen substantially with increasing system size and this change happens in a correlated way.

Eventually for $F_l \to \infty$ both kinds of curves might become constant for $\alpha > \alpha_c \simeq 1$. This would mean that the finite left–right gaps (whose existence was confirmed in section 4.1) would form a finite-dimensional subset. If true, this would be a novel quantitative characterization of the breakdown of translational invariance. This situation is analogous to the observation of Batrouni *et al* (1988) made in a study of random resistor networks. On this basis we conjecture the presence of a non-analyticity in $f(\alpha)$ at some α_c. This phenomenon is sometimes referred to as 'spectral phase transition' (see Benza and Callegaro 1990).

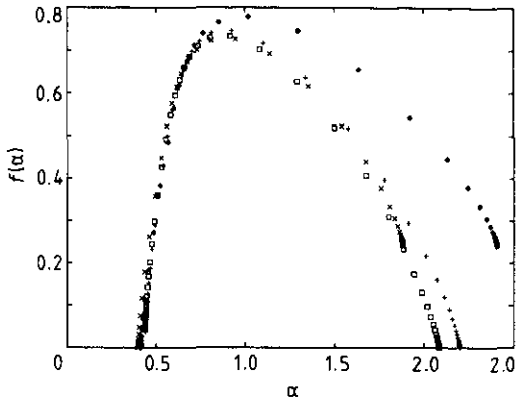

Figure 9. Finite-size effects in the distribution function $f(\alpha)$, for $r = 0.9$ and $Q = 0$ for the upper part of the one-fermion spectrum. The system sizes are $N =$ 2584: ◇, 1597: +, 987: □, 610: ×.

6. Conclusions

In this paper we have proposed a unified framework for the investigation of magnetic phase transitions in quasiperiodic systems. The study of the discrete energy levels of the critical quantum Ising model both in the even and in the odd sectors has revealed a characteristic pattern for the breakdown of translational invariance on finite approximants to quasiperiodic systems. The restoration of this symmetry was demonstrated both at the bottom of the spectrum and also at the edges of the largest gaps. A simple perturbative scheme was shown to describe quantitatively the most important features of the level structure. The multifractal analysis of the intra-doublet splittings yielded information on the distribution of scaling exponents.

Our qualitative understanding is satisfactory in a moderate neighbourhood of the periodic model. The study of the $r = 0.3$ case shows qualitatively new features, in particular for the higher excitations in the spectrum. For values of r close to zero, the model trivially decomposes into a large number of two- and three-sites systems. This tendency which charaterizes the $r = 0$ case is already apparent, for $r = 0.3$, for those states whose label is larger than F_{l-2}. The transition between the two parts of the level spectrum is clearly seen in the eigenvectors of the quantum Hamiltonian.

Acknowledgments

It is a pleasure to thank F Gähler for his help in analysing the Fourier spectrum of self-similar sequences and to thank M Droz and G Györgyi for helpful discussions. This work was partially supported by the Swiss National Science Foundation in the framework of the Programme of Cooperation with Eastern European Countries.

References

Ashcroft N W and Mermin N D 1976 *Solid State Physics* (Philandelphia, PA: Saunders) p 152
Aubry S, Godrèche C and Luck J-M 1988 *J. Stat. Phys.* **51** 1033
Batrouni G G, Hansen A and Roux S 1988 *Phys. Rev.* A **38** 3820
Benza V G 1989 *Europhys. Lett.* **8** 321
Benza V G and Callegaro V 1990 *J. Phys. A: Math. Gen.* **23** L841
Benza V G, Kolar M and Ali M K 1990 *Phys. Rev.* B **41** 9578

Cardy J L 1984 *J. Phys. A: Math. Gen.* **16** L385
Ceccatto H A 1989 *Z. Phys.* B **75** 253
Doria M M and Satija I 1988 *Phys. Rev. Lett.* **60** 444
Frachebourg L and Henkel M 1991 *J. Phys. A: Math. Gen.* **24** 5121
Gähler F 1991 to be published
Godrèche C and Luck J M 1990 *J. Phys. A: Math. Gen.* **23** 3769
Halsey T C, Jensen M H, Kadanoff L P, Procaccia I and Shraiman B I 1986 *Phys. Rev.* A **33** 1141
Henkel M 1990 *Finite Size Scaling and Numerical Simulation of Statistical Systems* ed V Privman (Singapore: World Scientific) ch VIII p 353
Henkel M and Patkós A 1987 *J. Phys. A: Math. Gen.* **20** 2199
Henkel M and Schütz G 1988 *J. Phys. A: Math. Gen.* **21** 2617
Iglói F 1988 *J. Phys. A: Math. Gen.* **21** L911
Kohmoto M, Sutherland B and Tang C 1987 *Phys. Rev.* B **35** 1020
Lieb E, Schultz T and Mattis D 1961 *Ann. Phys.* **16** 407
Luck J-M and Nieuwenhuizen Th M 1986 *Europhys. Lett.* **2** 257
McCoy B M and Wu T T 1973 *The Two-dimensional Ising Model* (Cambridge, MA: Harvard University Press)
Satija I 1990 *Phys. Rev.* B **41** 7235
Satija I and Doria M M 1988 *Phys. Rev.* B **38** 5174
Satija I and Doria M M 1989 *Phys. Rev.* B **39** 9757
You J Q, Zeng X, Xie T and Yan J R 1991 *Phys. Rev.* B **44** 713